Spatial integration for firm and load-following wind generation

López Prol, Javier; deLlano-Paz, Fernando; Calvo-Silvosa, Anxo; Pfenninger, Stefan; Staffell, Iain

DOI
10.1088/1748-9326/ad5d7d

Publication date
2024

Document Version
Final published version

Published in
Environmental Research Letters

IOP Publishing Environ. Res. Lett. 19 (2024) 094026 https://doi.org/10.1088/1748-9326/ad5d7d

ENVIRONMENTAL RESEARCH
LETTERS

OPEN ACCESS

RECEIVED
20 July 2023

REVISED
21 June 2024

ACCEPTED FOR PUBLICATION
1 July 2024

PUBLISHED
7 August 2024

LETTER

Spatial integration for firm and load-following wind generation

Javier López Prol[1], Fernando deLlano-Paz[2], Anxo Calvo-Silvosa[2], Stefan Pfenninger[3] and Iain Staffell[4,*]

1 Department of Economics, Yonsei University Mirae, Seoul, Republic of Korea
2 Business Department, University of A Coruña, A Coruña, Spain
3 Energy and Industry group, TU Delft, Delft, The Netherlands
4 Centre for Environmental Policy, Imperial College London, London, United Kingdom
* Author to whom any correspondence should be addressed.

E-mail: i.staffell@imperial.ac.uk and jlprol@yonsei.ac.kr

Keywords: energy transition, decarbonisation, transmission, variable renewable energy, wind power

Supplementary material for this article is available online

Abstract

Wind power has considerable potential to decarbonise electricity systems due to its low cost and wide availability. However, its variability is one factor limiting uptake. We propose a simple analytical framework to optimise the distribution of wind capacity across regions to achieve a maximally firm or load-following profile. We develop a novel dataset of simulated hourly wind capacity factors (CFs) with bias correction for 111 Chinese provinces, European countries and US states spanning ten years (∼10 million observations). This flexible framework allows for near-optimal analysis, integration of demand, and consideration of additional decision criteria without additional modelling. We find that spatial integration of wind resources optimising the distribution of capacities provides significant benefits in terms of higher CF or lower residual load and lower variability at sub-, quasi- and inter-continental levels. We employ the concept of firmness as achieving a reliable and certain generation profile and show that, in the best case, the intercontinental interconnection between China, Europe and the US could restrict wind CFs to within the range of 15%–40% for 99% of the time. Smaller configurations corresponding to existing electricity markets also provide more certain and reliable generation profiles than isolated individual regions.

1. Introduction

Wind power is one of the main instruments for decarbonising the energy sector. It is already one of the lowest-cost sources of electricity (Jansen *et al* 2020, IRENA 2022) with further predicted cost declines (Way *et al* 2022). Wind is expected to be the main source of electricity in 2050, accounting for 24% of global generation, according to the Net Zero report by the International Energy Agency (IEA 2021). However, the variability of wind (and solar) output means that clean firm technologies will be necessary to achieve rapid and cost-effective decarbonisation (Sepulveda *et al* 2018).

Wind variability poses challenges to its further diffusion: grid constraints, institutional factors and oversupply cause wind curtailment at moments of peak generation (Bird *et al* 2016, Drew *et al* 2019, Qi *et al* 2019, Xia *et al* 2020, López Prol and Zilberman 2023), the persistence of local low-wind events requires costly backup capacity or storage (Denholm and Hand 2011, Zerrahn and Schill 2017), and intermittency induces start-up costs to thermal power plants (Schill *et al* 2017). This variability imposes integration costs to the electricity system (Ueckerdt *et al* 2013, Hirth *et al* 2015, Joos and Staffell 2018, Reichenberg *et al* 2018), and the impact of high output lowering electricity prices, known as revenue cannibalisation, threatens the financial viability of variable renewables (Eising *et al* 2020, López Prol *et al* 2020, Liebensteiner and Naumann 2022).

Some solutions are already arising to address these problems. Storage and sector coupling could play a major role in renewables integration (Zerrahn *et al*

2018, Schmidt and Staffell 2023, López Prol and Schill 2021). Reducing the wind power inertia floor can reduce curtailment (Villamor *et al* 2020). Combining wind and solar provides complementarities (Schindler *et al* 2020, Solomon *et al* 2020, Costoya *et al* 2023, López Prol *et al* 2024). Geographic diversification (Mills and Wiser 2014) and internalising the external costs (Brown and Reichenberg 2021) of fossil fuels can mitigate and even reverse the cannibalisation effect. Large-scale electricity grids may also help integrating variable renewables (Grossmann *et al* 2015, Grams *et al* 2017, Aghahosseini *et al* 2019).

We propose the mean-variance framework, originally designed to obtain optimal investment portfolios in financial markets (Markowitz 1952), to quantify how the integration of different markets, optimising the distribution of wind capacity across regions, can achieve a firm and even load-following wind generation profile. Modern Portfolio Theory has been applied to energy markets, first to optimise fossil fuel procurement (Bar-Lev and Katz 1976) and later for a wide range of problems regarding technology selection and capacity allocation (DeLlano-Paz *et al* 2017). Particularly, this approach has been used to optimise wind allocation at different scales in Europe (Roques *et al* 2010) and China (Hu *et al* 2019).

We propose wind spatial integration across regions to achieve a 'firm' wind generation pattern that optimises the trade-off between achieving the maximum possible capacity factor (CF) with the lowest possible variability. We define 'firm wind' as the capacity of wind power to achieve a given level of *reliability*, in the sense of ensuring a minimum generation level for most of the time (e.g. 95% of hours with a CF above x), and *certainty*, understood as the concentration of the hourly CF distribution around a central reference value (e.g. mean CF ± 5 percentage points). We thus define 'Firmness' as a quantifiable continuum rather than a discrete characteristic of electricity generation technologies (Keane *et al* 2011).

Because demand also varies over time, achieving a flat generation profile is not sufficient to integrate high shares of variable renewables. For this reason, we demonstrate how this approach can be applied not only to CFs, but also to the difference between demand and wind generation, i.e. residual load. Reliability and certainty in this case can be analogously understood as having the minimum possible residual load with the minimum possible variability.

Our contribution is threefold: (i) we provide a new dataset including hourly CFs for 10 years (2010–19) for Chinese provinces, European countries and US states, totalling around 10 million observations; (ii) we propose a methodological implementation of demand within the mean-variance framework and a conceptual definition of firmness and load-following characteristics for variable renewables by combining the concepts of generation reliability and certainty. Using these new data, methods and definitions, (iii) we present the empirical results of optimal wind capacities across regions to obtain firm and load-following wind profiles and the resulting generation profiles and benefits of integration. Figure 1 summarises these contributions and their implementation.

2. Research design

First, we derive a novel dataset of hourly CFs for wind farms for China, Europe and the US covering a period of ten years (2010–19). We combine wind speeds from the ERA5 global reanalysis dataset (Hersbach *et al* 2020) with the Virtual Wind Farm model (Staffell and Green 2014), which is part of the Renewables.ninja platform (Pfenninger and Staffell 2016). We generate profiles of power generation for all known wind farms (both onshore and offshore) operating within China, Europe and the US as of January 2020. We then aggregate these site-specific simulations to regional aggregates (countries for Europe, provinces for China and states for the US, hereafter referred simply as regions), and then validate and bias-correct the simulations using a bespoke database of reported wind CFs from government sources (Staffell and Pfenninger 2016), ensuring that the resulting CFs are representative of real-world productivity. The final dataset comprises ∼10 million observations (89 280 hourly CF values for 111 regions, 32 in China, 29 in Europe and 51 in the US, see supplemental information for summary statistics).

Then, we use these data to optimise the CF-variability and the residual load-variability trade-offs at different integration levels: (i) *subcontinental* level according to existing electricity markets and power regions, (ii) *quasi-continental* level (China, Europe, and the contiguous US (i.e. excluding Alaska and Hawaii)), and (iii) *intercontinental* level linking these three areas. We compare these results with individual regions in autarky.

Wind CF is the ratio of actual to potential generation per unit of installed capacity, and variability is measured as the standard deviation (SD) of the hourly CF. We estimate the *portfolio*, i.e. the share of wind installed capacity per region, that minimises CF variability for each attainable mean CF for all considered spatial configurations. We show that increasing the geographical scope of the optimised systems improves their CF-variability trade-off. The largest system, the intercontinental interconnection between China, Europe, and the US provides the highest potential benefits, but smaller systems at sub- and quasi-continental levels also provide considerable potential benefits compared to individual regions in autarky. In summary, spatial integration

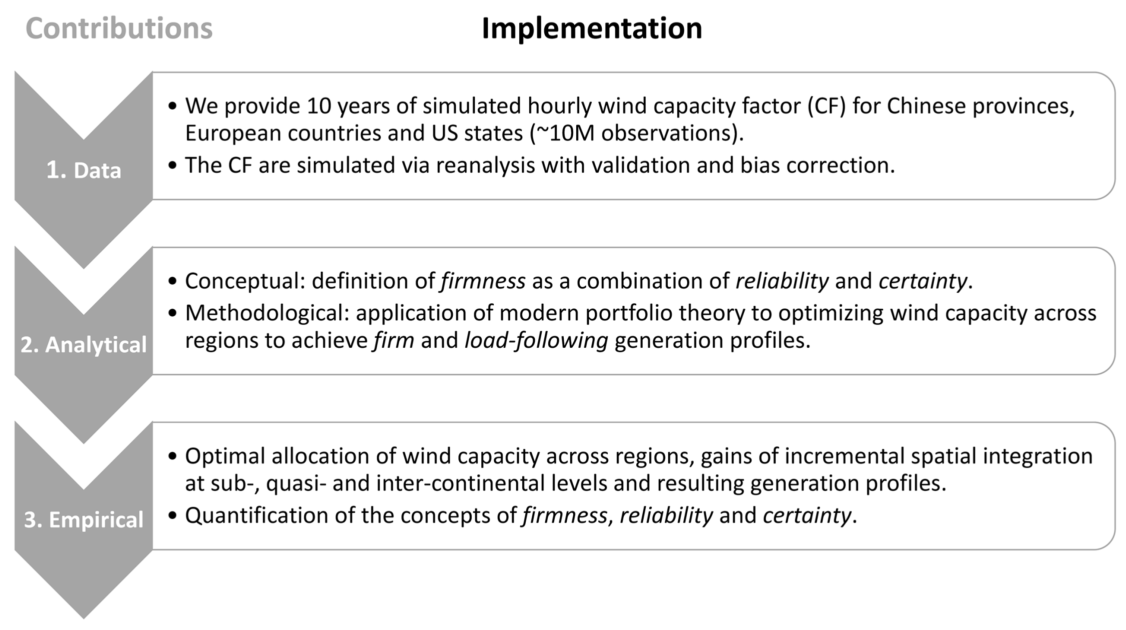

Figure 1. Summary of the research design including data generation, analytical and empirical contributions.

of regions with different generation patterns optimising the distribution of wind capacities provide a more reliable and certain aggregated generation pattern that can reduce curtailment, storage and backup capacity, enabling thus higher shares of wind power with lower integration costs.

2.1. Data generation

2.1.1. Wind speeds and power outputs

Wind speeds at 10 and 100 m above ground were extracted from the ERA5 reanalysis (Hersbach *et al* 2020). This was chosen over MERRA-2 as it is derived from a more recent model that assimilates more weather observations and delivers data with higher spatial resolution (0.25 × 0.25 degrees). Wind speeds at each timestamp and grid point were transformed into a log-law wind profile, which can infer wind speed, w, at any given turbine hub height, h, via:

$$w_h = A \log\left(\frac{h}{z}\right) \tag{1}$$

where A is the wind shear and z the surface roughness, derived from regression of the ERA5 wind speed data (Staffell and Green 2014). The resulting wind speeds were then interpolated spatially from the regular ERA5 grid to the location of individual wind farms using a non-smoothing spline.

Reanalysis has been shown to have bias in its wind speeds, which is reasonably stationary over time but heterogeneous across space (Decker *et al* 2012, Staffell and Pfenninger 2016). This means that while the pattern of wind farm production can be considered accurate, the long-term average level of production needs to be corrected according to the location. We apply a linear correction factor to wind speeds such that the resulting CFs match the observed long-run average at country, province or state level (Staffell and Pfenninger 2016). The correction combined a linear offset and multiplicative scale factor to provide an acceptable compromise between simplicity (thus avoiding over-fitting) and representing the seasonal and hourly variability across the regions studied.

Modified wind speed, w', was calculated from raw wind speed, w, and the bias—or systematic error—in CFs, which is defined as the ratio of observed to simulated capacity factors, CF:

$$w' = \left(0.6\,\frac{\mathrm{CF_{obs}}}{\mathrm{CF_{sim}}} + 0.2\right) w + \beta. \tag{2}$$

For each individual wind farm, the VWF model uses a simple iterative process to seek a value for linear offset term, β, so that the farm's long run average CF is scaled by the desired bias correction factor, $\frac{\mathrm{CF_{obs}}}{\mathrm{CF_{sim}}}$. The ratio of multiplicative and additive components (0.6 and 0.2 in the above equation) are taken from previous work (Staffell and Pfenninger 2016).

Wind speeds were converted to power outputs using empirical power curves that were collected for 140 models of wind turbine (Pfenninger and Staffell 2016). These curves were smoothed using a Gaussian kernel to account for the distribution of wind speeds experienced within any given hour, and between the individual turbines of a specific farm (Staffell and Pfenninger 2016).

2.1.2. Wind farm simulations

We modelled all wind farms that were known to be operating in each region we consider as of January 2020. For this, we took the location (latitude and longitude), hub height (in metres), installed capacity (in

MW) and the model of wind turbine for each farm from The Wind Power database (Pierrot 2023). This yielded 1180 wind farms in China, 1442 in the US and 19 979 in Europe.

Missing metadata for these farms were inferred where possible. Latitude and longitude data were missing for 5% of farms (14% in China, 2% in the US, 5% in Europe). These were inferred by geolocation where the nearest county or city was known using the Bing Maps Locations API[5]. Hub height data were missing for 37% of wind farms (80% in China, 26% in the US and 35% in Europe). These were inferred by stochastically sampling other wind farms with known heights that use the same turbine model in the same country or neighbouring countries if none were available. Turbine model was not known for 20% of wind farms (11% in China, 21% in the US and 20% in Europe). These were inferred by stochastically sampling other wind farms with similar capacity, average estimated wind speed and construction date in the same country or neighbouring countries if none were available.

Despite simulating the output of over 20 000 wind farms, there were some regions in this study with limited coverage; for example, no wind farms were specified in the US states of Alabama, Louisiana or Florida. We therefore randomly generated hypothetical wind farms in any region which contained fewer than 20 wind farms, and add these to the known farms so that at least 20 sites were modelled within each region. This number was chosen so that each hypothetical turbines could not substantially influence results, as each would contribute at most 5% to the region's overall profile. These farms were randomly placed within the region, with randomly selected turbine model and hub height sampled from other farms within the country or neighbouring countries. They were given a negligible capacity (a single turbine, typically 1–6 MW) so their output would only affect regions with little to no existing wind farms, and thus add some geographical diversity to their regional aggregate. This process was applied to 14 Chinese provinces (BJ, CQ, GX, GZ, HA, HE, HN, HU, JX, QH, SA, SC, TJ, XZ) and 28 US states (AL, AR, AZ, CT, DC, DE, FL, GA, HI, KY, LA, MD, MO, MS, MT, NC, NH, NJ, NV, RI, SC, SD, TN, UT, VA, VT, WI, WV) which each had fewer than 20 farms (see supplementary tables 3 and 4 for full names of these regions). Across these 14 Chinese provinces, hypothetical turbines represented 19% of installed capacity (2.6% across the whole of China). Across these 28 US states, hypothetical turbines represented 23% of installed capacity (1.9% across the whole of the United States). These provinces and states contribute little or nothing to the optimal portfolios found in this work (e.g. see figure 2 later), as they have lower CFs with higher variability (hence few developers have chosen to install wind farms there to date).

The resulting wind farm simulations were aggregated to give the time series of total power output at national level in Europe, state level in the US and provincial level in China. The GADM dataset level 0 and level 1 were used to define the shapefile for each region. One exception to this was that the Chinese province of Nei Mongol (Inner Mongolia) was further separated into an eastern and western region due to its importance for wind power production and physical size (spanning almost 30 degrees of longitude). This split was defined by banner/county-level administrative divisions, with those to the west of Abag and Plain Blue defined as West Nei Mongol, and those east of (and including) them as East Nei Mongol.

2.1.3. Validation and bias correction

We update previous bias correction factors for European countries (Staffell and Pfenninger 2016) and replicate their calculations for Chinese provinces and US states. Bias correction factors for all regions are given in the supplementary information. For Europe, hourly metered wind farm output was collected from the ENTSO-E Transparency Platform[6] and national transmission system operators (TSOs) in 12 countries, plus annual-average CFs derived from IRENA[7] for the remaining countries.

The only public data found for China were annual average CFs for each province, published by the National Energy Administration from 2013 to 2019[8]. Wind farm curtailment due to grid constraints is an important consideration, as this amounted to 17% of all wind power production across China in 2016, falling to 4% in 2019[9]. This was removed from the data to give gross CFs (i.e. what could have been attained given the prevailing meteorological conditions).

Monthly-average CFs were derived for US states from the Electric Power Monthly dataset published by the Energy Information Administration[10]. This covered 36 states which had at least 10 MW of wind capacity installed and at least three years of reported data.

2.2. Portfolio optimisation

2.2.1. Modern portfolio theory

We apply Modern Portfolio Theory to assess the trade-off between CF and variability (measured as SD) for wind generation. We use the hourly wind CF data for each region during 10 years presented

[5] https://docs.microsoft.com/en-us/bingmaps/rest-services/locations/.

[6] https://transparency.entsoe.eu/.

[7] https://www.irena.org/Data.

[8] www.nea.gov.cn/2020-02/28/c_138827910.htm.

[9] www.nea.gov.cn/2020-02/28/c_138827910.htm.

[10] www.eia.gov/electricity/data/state/.

above. The problem consists in minimising the portfolio SD (σ_p) for the attainable range of average capacity according to equation (1):

$$\min(\sigma_p) = \min\left(\sqrt{\sum_i w_i^2\sigma_i^2 + \sum_i\sum_{j\neq i} w_i w_j \rho_{ij}\sigma_i\sigma_j}\right) \tag{3}$$

where the first addend is the sum of variances (σ_i^2) times the squared shares of wind installed capacity in each country (w_i^2) and the second addend is the covariance of hourly CF between regions and their correlation ρ_{ij}. This minimisation is subject to a non-negativity constraint (i.e. all shares must be positive or zero: $w_i \in \mathbb{R} \geqslant 0$), and a 'full investment' constraint (i.e. the sum of shares must equal one, $\sum w_i = 1$). This process is iterated for all attainable levels of the CF, such that each iteration includes the constraint that the portfolio CF must be equal to a value exogenously set $(\sum \frac{w_i\,\overline{\mathrm{CF}}_i}{w_i} = \mathrm{CF})$. The result of this optimisation exercise is a set of efficient portfolios that have the minimum possible variability for each attainable mean CF. Each portfolio is the relative distribution of wind installed capacities across regions, as shown in the maps in figures 2 and 3. Finally, we obtain the optimal portfolio for each configuration as the one that maximises the mean CF per unit of variability, which is the inverse of the coefficient of variation: $\mathrm{CV}^{-1} = \overline{\mathrm{CF}}/\mathrm{SD}$.

2.2.2. Levelised cost of electricity (LCOE)

The LCOE in figure 2 panels A1–A3 is calculated with the simplified formula:

$$\mathrm{LCOE} = \frac{\mathrm{IC}\cdot\mathrm{CRF} + \mathrm{O\&M}}{\mathrm{CF}\cdot 8760} \tag{4}$$

$$\mathrm{CRF} = \frac{i(1+i)^n}{(1+i)^n - 1} \tag{5}$$

where CRF is the capital recovery factor, which depends on the interest rate i (assumed 5%) and the lifetime of the system n (assumed 25 years). We assume a discount rate of $i = 5\%$, taken from the weighted average cost of capital in 2020 for the OECD and China (IRENA 2022). The installation cost (IC) is assumed to be \$1325/kW corresponding to the global weighted average as reported by the latest IRENA cost report (IRENA 2022). IRENA reports operation and maintenance costs ranging between 33–50 \$/kW annually, so we assume an intermediate value of \$40/kW per year. The CF corresponds to each regional value in figure 2. These cost assumptions are used for illustrative purposes and are equal across all regions, so they do not affect the distribution of capacity across regions. More granular cost data (e.g. from Hatton *et al* 2024) could be used instead to reflect regional differences.

3. Benefits of integration

Figure 2 shows the potential benefits of spatial integration in optimising the trade-off between high CF and low variability at different integration levels. Grey dots indicate the mean CF and SD for each region in autarky at hourly level across the 10 years (2010–2019). The resulting CF determines the LCOE for a given IC. The right vertical axes of figure 2, panels A1–A3 show the range of LCOE assuming 2021 global weighted average onshore wind costs (IRENA 2022) and using the simplified LCOE calculation (see methods). supplementary figure 1 presents additional summary statistics including coefficients of variation $(\mathrm{CV} = \mathrm{SD}/\overline{\mathrm{CF}})$ per region, showing that smaller regions usually present lower CF and higher CV because larger regions already benefit from some of the effects of spatial integration described below.

We define the subcontinental spatial configurations according to the existing electricity markets and power regions in China, Europe and the US (see the maps in figure 2 and the complete list in section 4 of the supplementary information). We then optimise the portfolio of wind installed capacity for each configuration that minimises variability (SD) for each attainable level of CF. Figure 2 panels A1–A3 show the benefits of integration and coordination of each configuration at the sub- and quasi-continental levels with respect to regions in autarky. The efficient frontiers (coloured lines) represent the set of portfolios that minimise variability for each attainable mean CF. The highlighted coloured point on each frontier represents the portfolio that optimises this trade-off in terms of achieving the maximum possible mean CF per unit of variability, i.e. the reciprocal of the coefficient of variation $(\mathrm{CV}^{-1} = \overline{\mathrm{CF}}/\mathrm{SD})$. Whereas this portfolio is the technical optimum, this approach provides decision-makers room to move along the frontier to keep efficient configurations depending on their preferences regarding the levels of CF (determining LCOE) and variability (determining integration costs), as well as other potential complementary capacity allocation criteria. This framework also provides the feasible space below the efficient frontier to assess second-best options along the lines of the near-optimal energy modelling reasoning (Neumann and Brown 2021).

The lower-left corner of the frontier is the portfolio with the lowest possible variability (see supplementary figure 3). As we move up and rightwards along the frontier, we prioritise higher CF over lower variability up to the maximum possible CF at the top right of the frontier. The decision of where to move along the curve will ultimately depend on the balance between the cost of variability and the value of generation. This is a fertile avenue of further research to expand this approach depending on different cost/value assumptions or additional capacity

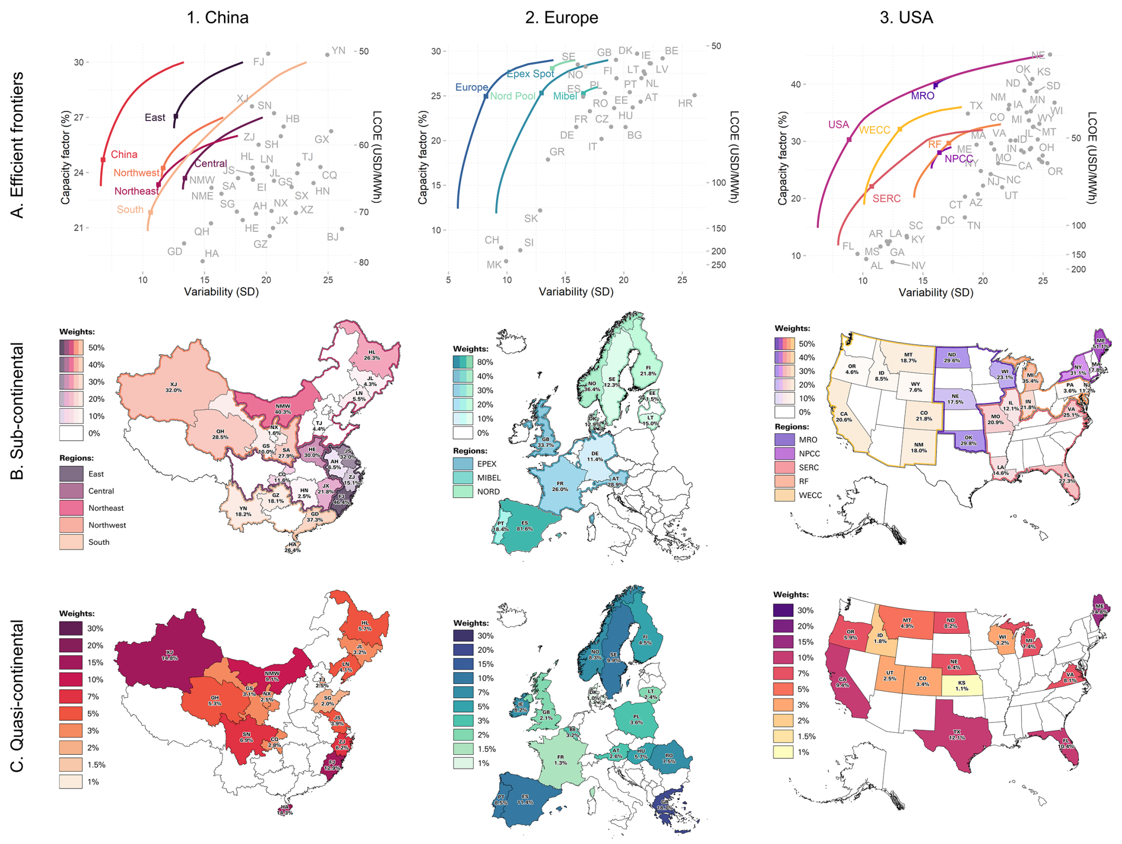

Figure 2. Spatial integration and deployment coordination improve the capacity factor-variability trade-off with respect to any single region in autarky. Panels A1–A3: grey points indicate the mean capacity factor and variability (measured as the standard deviation of the hourly capacity factor, in percentage) for each Chinese province, European country and US state in autarky. Lines represent the efficient frontiers, where each point along the frontier is a portfolio of shares of installed wind capacity per region with the minimum possible variability for each mean capacity factor. The highlighted points along the frontiers indicate the optimal portfolio (defined as the maximum mean capacity factor per unit of variability). The assumptions for the calculation of the levelised cost of electricity (LCOE in USD/MWh, right axis) are $1325/KW installation cost, $40/KW yearly operation and maintenance cost, 25 years lifetime and 5% interest rate. Note that the panels have different axes scales and the relation between CF (left axis) and LCOE (right axis) is nonlinear. Panels B1–B3 give the optimal portfolio for each sub-continental configuration, and panels C1–C3 give the optimal quasi-continental configurations. In panels B1–B3, each power region is represented by a different colour and surrounded by a thick border, and the colour intensity of each region (province, country or state) represents the share of wind installed capacity relative to the larger power region to which it belongs. See supplementary figure 3 for the minimum variability portfolios the list of regions in section 4 of the supplementary information.

allocation criteria and constraints. For now, we focus on the technical optimum (i.e. the maximum attainable mean CF per unit of variability), as it provides the foundations to achieve a firm wind generation pattern that provides high levels of reliability and certainty.

Whereas we focus here on the technical optimum (point along the frontier), any portfolio of shares along the efficient frontier can be obtained from the code and data made available by the authors (see data availability section Prol *et al* 2023). Supplementary figure 3 shows the installed capacities for the minimum variability portfolio (bottom-left corner of the efficient frontier). In this case, capacities are located in the regions with opposite generation patterns to achieve the flattest possible aggregate generation profile.

The efficient frontiers in panels A1–A3 of figure 2 show that even small configurations at sub-continental level provide significant benefits in terms of higher CFs and lower variability compared to individual regions in autarky. These configurations are relatively easier to implement in reality because these power regions already have some level of integration. Continental-scale integration and coordination is always better than smaller sub-continental configurations. The case of Mibel (the Iberian Electricity Market) exemplifies the basic functioning of this framework. Since it comprises only two countries (Portugal and Spain), the frontier is roughly a line between both countries (representing all possible capacity allocation options between both countries), and the benefits from integration and coordination are limited because both countries have similar generation patterns. As the configurations become larger and more diverse in terms of generation patterns, the efficient frontiers shift left and upwards, indicating lower variability and higher CF, respectively, and thus higher potential gains. The maps in figure 2 show the optimal shares of wind installed capacity

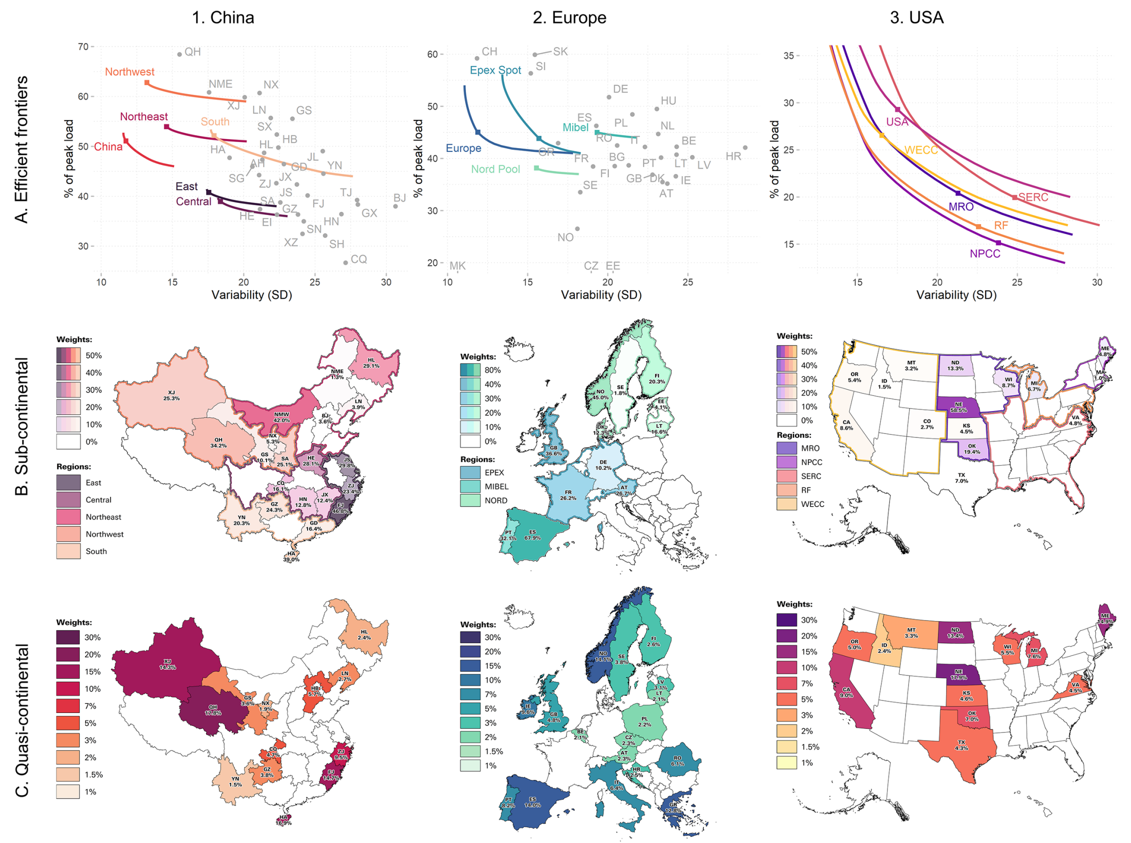

Figure 3. Residual load efficient frontiers (as % of peak load) for (1) China, (2) Europe and the (3) US. Grey dots represent regions in autarky. Lines show the efficient frontier of portfolios with the minimum possible variability for each level of residual load. The highlighted point on the frontiers shows the portfolio with the lowest product of residual load and variability. See supplementary figure 11 for the analogous figure for the minimum variability portfolios.

for the sub-continental (panels B1–B3) and quasi-continental (panels C1–C3) configurations.

Supplementary figure 2 presents the same analysis for a hypothetical intercontinental configuration between China, Europe and the US. Recent studies show the feasibility of intercontinental interconnections with ultra-high-voltage transmission lines (Guo *et al* 2022) and multiple projects are currently being planned (e.g. Xlinks between Morocco and the UK or the Australia-Asia Power Link), although other studies question their profitability (Reichenberg *et al* 2022).

4. Load-following wind

We have so far focused on the supply side by studying the trade-off between CF and production variability. Minimising residual load and its variability, however, would in principle be preferable than just maximising CF for each level of variability. By integrating demand in our analysis, we can obtain 'load-following' wind power by minimising residual load, rather than just 'firm wind' by maximising CF.

The 'load-following' empirical results are not likely to hold in the future as demand patterns are expected to change dramatically due to electrification, sector coupling and demand flexibility (Hostick *et al* 2014). For this reason, we illustrate here the approach with current available demand data for 2019 (Crozier and Baker 2022), but further research should derive long-term empirical results with future demand patterns.

Demand data for the US are not available at the state level, but only for 13 regions (California, Carolinas, Central, Florida, Mid-Atlantic, Midwest, New England, New York, Northwest, Southeast, Southwest, Tennessee and Texas). We aggregate them at the power region level such that WECC comprises California, Northwest and Southwest, SERC includes Carolinas, Florida, Southeast and Tennessee), RF corresponds to Mid-Atlantic, NPCC is formed by New England and New York and ERCOT is Texas. Finally, because the Midwest region belongs to multiple different power regions, we assigned the population-weighted shares of demand to each power region, such that (i) Louisiana, Arkansas, Missouri and Illinois, accounting for 45.9% of the total Midwest region, are assigned to SERC, (ii) Indiana and Michigan, accounting for 28.9% of the total, are assigned to RF, and (iii) Iowa, Wisconsin and Minessota, accounting for 25.2% of the total, are assigned to MRO. For this reason, autarky results for US states are omitted from this analysis.

We first express demand normalised against peak demand ($D_t / \max(D_t)$) for each region to have comparable results across regions with very different consumption levels. Then we calculate hourly residual load (RL_t) as the difference between demand (expressed as a share of peak load) and the CF (CF_t). This is equivalent to assuming that we install the same wind capacity as peak load. Thus, positive RL values mean residual loads that should be met by other means, and negative ones mean that wind generation is higher than load:

$$\mathrm{RL}_t = \frac{D_t}{\max(D_t)} - \mathrm{CF}_t. \tag{6}$$

We replicate this process for all configurations, such that we first aggregate demand within the system and then calculate the peak and residual loads. The problem is then analogous as with the CF: we want to find the efficient frontier of portfolios that provide the minimum possible portfolio variability for each level of attainable residual load (see methods section).

Figure 3 is the load-following analogous to the firm wind results presented in figure 2. Figure 3 thus shows the average residual demand for each region of each continent and its SD in autarky. The negative value for Estonia means that if Estonia installed as much wind capacity as its peak load, it would have an average of 20% excess generation. Positive values represent the remaining residual load, that could be met by other means or by installing more capacity than the peak load. The efficient frontiers are now downward-sloping because we minimise residual load in the vertical axis instead of maximising CF. Integration benefits are harder to see because they are confounded by different demand patterns across countries. For example, if one single country has a positive correlation between generation and demand, its residual load in autarky may look better than when integrated with other countries with a negative generation-demand correlation despite the fact that integration provides net benefits overall. This is the reason why larger spatial configuration efficient frontiers are not necessarily lower (i.e. better) than smaller ones in figure 3.

Whereas the optimal capacities shown in figures 2 and 3 optimise the trade-off between CF/residual load and variability, respectively, they do not represent the actual optimal capacities, as this simple model misses the interactions with other generation and storage technologies and the different costs across regions. Constraints on minimum and maximum capacities could be exogenously imposed to obtain more realistic results.

The firm wind results are more empirically relevant because demand patterns will change in the future and provide a cleaner conceptualisation of gains because different demand-generation correlations across countries confound the final results for the case of residual load. For these reasons, we focus the remainder of this paper on the operationalisation of the concept of 'firmness', but the analogous analysis for load-following wind is provided in the supplementary information.

5. Firm wind

We define the 'firmness' of wind power as the capacity to provide the highest possible level of reliability and certainty. To assess the implications of our results we further operationalise these definitions by specifying *reliability* as the capacity to provide a minimum CF for 95% of the time, and certainty as the probability of CFs within the range of the mean CF ±5 percentage points. These values are arbitrarily chosen to resemble the conventional 5% significance levels commonly used in statistics, but any other value could be used, see supplementary figure 4 for the same illustration with the levels of 1%/±1p.p. and 10%/±10p.p.. Figure 4(A) shows the level of firmness for each region in autarky (grey) and configuration according to these definitions. Individual regions in autarky provide low reliability and certainty (lower-left corner), but as regions integrate optimising the distribution of wind capacities, reliability and certainty increase (upper-right corner) until achieving 95% of hours with a CF above 19% and 70% of hours with a CF within the range 21%–31% (26% mean ± 5p.p.) in the intercontinental configuration. The quasi-continental configurations obtain levels of reliability between 13%–16% with higher than 40% certainty, and all subcontinental configurations perform better than any region in autarky.

Another way to operationalise these definitions is by looking at the CF cumulative distribution functions (figure 4(B)). The CF cumulative distribution functions show how optimised portfolios improve certainty and reliability, achieving thus firmer generation profiles. The slope of the cumulative distribution function shows how concentrated hourly CFs of the optimal portfolios are around the central values, showing therefore how certain its generation pattern is. Likewise, reliability is the capacity to provide a minimum level of generation all or most of the time. Cumulative distribution functions that start flat at 0 and are more displaced to the right are more reliable because the probability of low CFs is lower. For instance, Nebraska's CF interquartile range is 23%–67%. While its mean CF is high (45%), its generation pattern is uncertain due to a large interquartile spread (43 percentage points (p.p.)), and unreliable because the CF is lower than 10% almost 9% of the time. In the other extreme, Switzerland has a certain but unreliable generation pattern. Wind spatial integration and deployment coordination across the contiguous US would

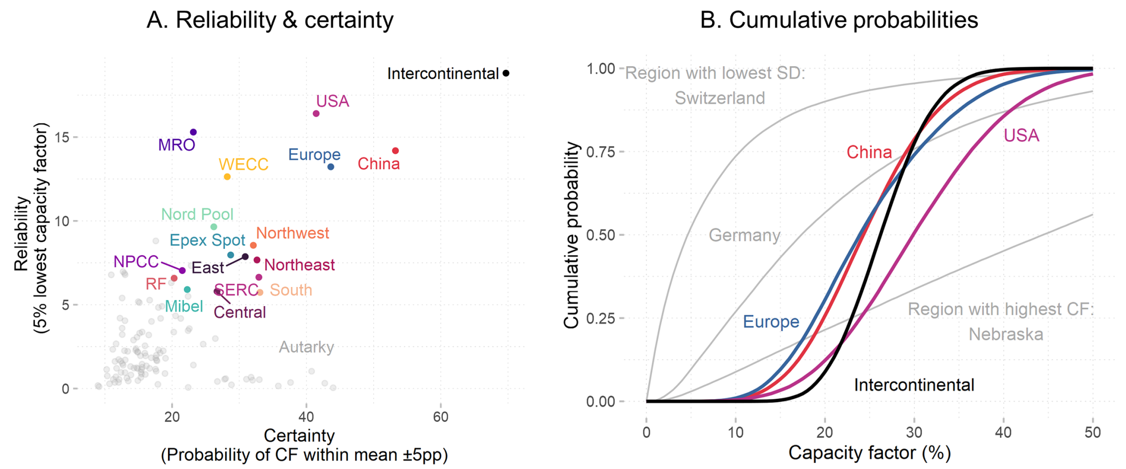

Figure 4. Firm wind. (A) Wind reliability, measured as the minimum capacity factor (CF) achieved 95% of the time (i.e. the 5th percentile of the CF), and certainty, measured as probability of CF within the mean ±5 percentage points. See supplementary figure 5 for the same figure at other levels of reliability and certainty, and supplementary figure 9 for the analogous analysis of residual load. (B) Capacity factor cumulative probability for each quasi-continental and the intercontinental configurations and selected regions.

improve both certainty (interquartile range spread declines to 12p.p. [24%–36% CF]) and reliability (CF lower than 10% only 0.4% of the time), at the cost of a lower mean CF (30%). An intercontinental configuration improves reliability and certainty even further, achieving a CF between 15%–40% for 99% of the time (interquartile range spread of only 7p.p. (23%–30% CF) and a minimum CF of 9%). Thus, even regions with high mean CFs can benefit from spatial integration (see supplementary table 1 for the summary statistics of the optimised generation profiles for all configurations).

Finally, figure 5 compares the resulting aggregate generation profiles (10 year average and SD) of the optimised portfolios (left column) with selected regions in autarky (right column). The first row shows the optimal intercontinental wind generation profile compared to Switzerland, the region with the lowest variability of the dataset. The optimal intercontinental profile provides both a higher mean CF and lower variability than even the region with lowest variability. The other rows compare the optimal quasi-continental portfolios with the region with the highest CF of each configuration. The optimal quasi-continental profiles will have, by definition, a lower mean CF than the region with the highest CF of each configuration, but in return have a much 'firmer' generation profile that resembles a baseload technology.

6. Conclusions

We show that the spatial integration of wind resources can bring substantial benefits in optimising the trade-off between high CFs (or low residual load) and low variability. This can help mitigate integration costs and the cannibalisation effect, and reduce the need for backup capacity and curtailment. Wind power can provide a considerable level of 'firmness', defined as combination of *reliability* (a minimum level of generation most of the time) and *certainty* (CF distribution concentrated around a central value). When including demand in the analysis, we show that spatial integration can minimise residual load and its variability providing a wind generation profiles that approaches the demand pattern.

The main advantage of this approach is its simplicity and flexibility. Simplicity because it only requires data on hourly CF (and demand for the load-following approach) and a basic optimisation method. With the proposed definitions of reliability and certainty, this approach allows us to compare the 'firmness' of different portfolios (shares of installed capacities across countries) and the potential gains from system integration and deployment coordination. Flexibility because it allows the comparison between many different portfolios, optimal (maximum CF per unit of variability), efficient (along the frontier) or any other near-optimal (below (above for the load-following approach) the frontier) alternatives.

The simplicity of this approach is also its main limitation. Because it only considers wind, it ignores the interactions with other generation or storage technologies. The results represent the technical optima, but because we ignore cost differences across countries, it does not necessarily coincide with the economic optima. Future extensions could integrate capacity and integration costs for the firm wind approach, and backup cost for the load-following approach. Likewise, transmission cost could be considered to complete the cost-benefit analysis.

The mean-variance framework has several limitations, such as (i) the instability of the portfolio shares, (ii) the problem of using past data to make long-term

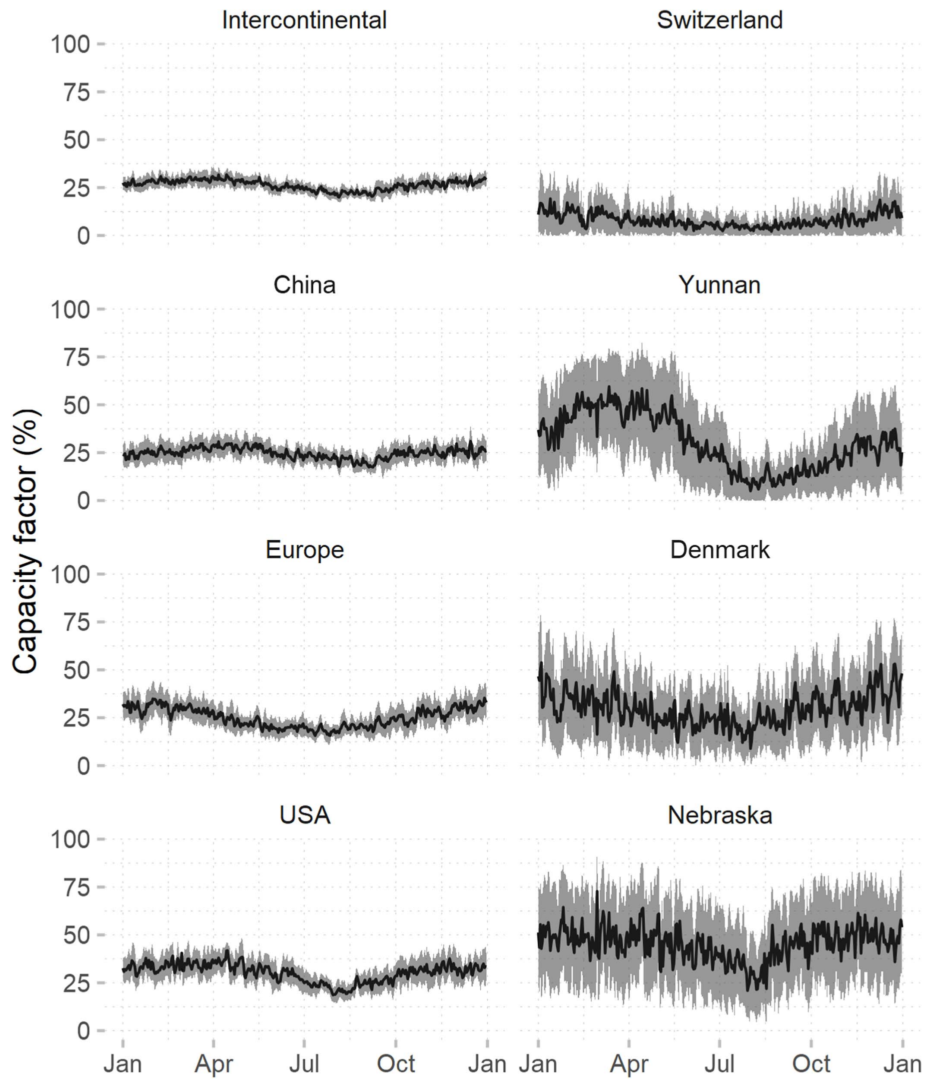

Figure 5. Capacity factor profiles of the optimised intercontinental and quasi-continental configurations (left column) compared to the region with lowest standard deviation of the dataset (Switzerland), and with the regions with the highest capacity factor within each quasi-continental configuration. The solid line is the 10 year average and the shaded area is the standard deviation. See supplementary figure 10 for the analogous analysis of residual load.

future decisions, and (iii) giving equal consideration to upside and downside variability. Potential improvements for further research include (i) assessing no-regret second-best shares (i.e. allocations that may not be optimal but are robust to different types of uncertainty), (ii) integrating projections of technology evolution and potential changes in weather and demand patterns, and (iii) applying measures of downside risk instead of variability as proposed by post-modern portfolio theory.

Practically achieving the proposed levels of international interconnection and coordinated deployment, however, depends on both institutional factors and the costs of spatial integration (mainly interconnections), compared to alternative flexibility options, such as storage, demand management or zero-carbon dispatchable technologies. Spatial integration has co-benefits related to the integration of other variable renewable energy technologies (mainly solar), the balance of different consumption patterns and grid resilience more generally, but also risks associated with energy interdependence between countries. Further research should take all these aspects into account to assess the economic and political feasibility of international interconnections. Plans in this direction are already being discussed in China (Fairly 2019), Europe (European Commission 2017) and the US (Bloom *et al* 2020).

Data availability statement

The code and data that support the findings of this study are openly available at the following URL/DOI: https://doi.org/10.5281/zenodo.7725407.

Acknowledgments

J L P gratefully acknowledges the support of the Green Finance Specialist Education and Training Program of the Korea Ministry of Environment, which partially funded this research. S P and I S were funded through the European Union's Horizon 2020 research and innovation programme under Grant Agreement No. 837089. I S also acknowledges support from EPSRC via EP/R045518/1.

Author contributions

Javier López Prol: Conceptualization, Formal analysis, Writing—Original Draft, Writing—Review & Editing, Visualization, Supervision, Project administration.

Iain Staffell: Resources, Formal analysis, Visualization, Writing—Review & Editing.

Stefan Pfenninger: Resources, Formal analysis, Writing—Review & Editing.

Fernando de Llano Paz: Conceptualization, Writing—Review & Editing.

Anxo Calvo Silvosa: Conceptualization, Writing—Review & Editing.

Conflict of interest

The authors declare no competing interests.

ORCID iDs

Javier López Prol https://orcid.org/0000-0001-6654-8405
Fernando deLlano-Paz https://orcid.org/0000-0003-1008-2284
Anxo Calvo-Silvosa https://orcid.org/0000-0001-7760-7845
Stefan Pfenninger https://orcid.org/0000-0002-8420-9498
Iain Staffell https://orcid.org/0000-0003-1012-7075

References

Aghahosseini A, Bogdanov D, Barbosa L S N S and Breyer C 2019 Analysing the feasibility of powering the Americas with renewable energy and inter-regional grid interconnections by 2030 *Renew. Sustain. Energy Rev.* **105** 187–205

Bar-Lev D and Katz S 1976 A portfolio approach to fossil fuel procurement in the electric utility industry *J. Finance* **31** 933

Bird L *et al* 2016 Wind and solar energy curtailment: a review of international experience *Renew. Sustain. Energy Rev.* **65** 577–86

Bloom A *et al* 2020 *The Value of Increased HVDC Capacity between Eastern and Western U.S. Grids: The Interconnections Seam Study* (NREL Prepr)

Brown T and Reichenberg L 2021 Decreasing market value of variable renewables can be avoided by policy action *Energy Econ.* **100** 105354

Costoya X, deCastro M, Carvalho D and Gómez-Gesteira M 2023 Assessing the complementarity of future hybrid wind and solar photovoltaic energy resources for North America *Renew. Sustain. Energy Rev.* **173** 113101

Crozier C and Baker K 2022 The effect of renewable electricity generation on the value of cross-border interconnection *Appl. Energy* **324** 119717

Decker M, Brunke M A, Wang Z, Sakaguchi K, Zeng X and Bosilovich M G 2012 Evaluation of the reanalysis products from GSFC, NCEP, and ECMWF using flux tower observations *J. Clim.* **25** 1916–44

DeLlano-Paz F, Calvo-Silvosa A, Antelo S I and Soares I 2017 Energy planning and modern portfolio theory: a review *Renew. Sustain. Energy Rev.* **77** 636–51

Denholm P and Hand M 2011 Grid flexibility and storage required to achieve very high penetration of variable renewable electricity *Energy Policy* **39** 1817–30

Drew D R, Coker P J, Bloomfield H C, Brayshaw D J, Barlow J F and Richards A 2019 Sunny windy sundays *Renew. Energy* **138** 870–5

Eising M, Hobbie H and Möst D 2020 Future wind and solar power market values in Germany—evidence of spatial and technological dependencies? *Energy Econ.* **86** 104638

European Commission 2017 *Towards a sustainable and integrated Europe* (Report of the Commission Expert Group on electricity interconnection targets)

Fairly P 2019 China's ambitious plan to build the world's biggest supergrid (IEEE Spectr) (available at: https://spectrum.ieee.org/chinas-ambitious-plan-to-build-the-worlds-biggest-supergrid) (Accessed 9 July 2021)

Grams C M, Beerli R, Pfenninger S, Staffell I and Wernli H 2017 Balancing Europe's wind-power output through spatial deployment informed by weather regimes *Nat. Clim. Change* **7** 557–62

Grossmann W, Grossmann I and Steininger K W 2015 Solar electricity supply isolines of generation capacity and storage *Proc. Natl Acad. Sci. USA* **112** 3663–8

Guo F *et al* 2022 Implications of intercontinental renewable electricity trade for energy systems and emissions *Nat. Energy* **7** 1–13

Hatton L, Johnson N, Dixon L, Mosongo B, De Kock S, Marquard A, Howells M and Staffell I 2024 The global and national energy systems techno-economic (GNESTE) database: cost and performance data for electricity generation and storage technologies *Data Brief* **55** 110669

Hersbach H *et al* 2020 The ERA5 global reanalysis *Q. J. R. Meteorol. Soc.* **146** 1999–2049

Hirth L, Ueckerdt F and Edenhofer O 2015 Integration costs revisited—an economic framework for wind and solar variability *Renew. Energy* **74** 925–39

Hostick D, Belzer D, Hadley S, Markel T and Marnay C 2014 *Projecting Electricity Demand in 2050* (Pacific Northwest Natl. Lab. PNNL)

Hu J, Harmsen R, Crijns-Graus W and Worrell E 2019 Geographical optimization of variable renewable energy capacity in China using modern portfolio theory *Appl. Energy* **253** 113614

IEA 2021 Net zero by 2050 a roadmap for the global energy sector

IRENA 2022 Renewable power generation costs in 2021

Jansen M, Staffell I, Kitzing L, Quoilin S, Wiggelinkhuizen E, Bulder B, Riepin I and Müsgens F 2020 Offshore wind competitiveness in mature markets without subsidy *Nat. Energy* **5** 614–22

Joos M and Staffell I 2018 Short-term integration costs of variable renewable energy: wind curtailment and balancing in Britain and Germany *Renew. Sustain. Energy Rev.* **86** 45–65

Keane A, Milligan M, Dent C J, Hasche B, D'Annunzio C, Dragoon K, Holttinen H, Samaan N, Söder L and O'Malley M 2011 Capacity value of wind power *IEEE Trans. Power Syst.* **26** 564–72

Liebensteiner M and Naumann F 2022 Can carbon pricing counteract renewable energies' cannibalization problem? *Energy Econ.* **115** 106345

López Prol J, de Llano Paz F, Calvo Silvosa A, Pfenninger S and Staffell I 2024 Wind-solar technological, spatial and temporal complementarities in Europe: a portfolio approach *Energy* **292** 130348

López Prol J and Schill W-P 2021 The economics of variable renewable energy and electricity storage *Annu. Rev. Resour. Econ.* **13** 443–67

López Prol J, Steininger K W and Zilberman D 2020 The cannibalization effect of wind and solar in the California wholesale electricity market *Energy Econ.* **85** 104552

López Prol J and Zilberman D 2023 No alarms and no surprises: dynamics of renewable energy curtailment in California *Energy Econ.* **126** 106974

Markowitz H 1952 Portfolio Selection *J. Finance* **7** 77

Mills A and Wiser R 2014 Strategies for mitigating the reduction in economic value of variable generation with increasing penetration levels *Ernest Orlando Lawrence Berkeley Natl. Lab.* **36** 119–27

Neumann F and Brown T 2021 The near-optimal feasible space of a renewable power system model *Electr. Power Syst. Res.* **190** 106690

Pfenninger S and Staffell I 2016 Long-term patterns of European PV output using 30 years of validated hourly reanalysis and satellite data *Energy* **114** 1251–65

Pierrot M 2023 Wind energy database (available at: www.thewindpower.net/) (Accessed 9 July 2023)

Prol J L *et al* 2023 Spatial integration and deployment coordination for firm wind generation *Zenodo* (https://doi.org/10.5281/zenodo.7725407)

Qi Y, Dong W, Dong C and Huang C 2019 Understanding institutional barriers for wind curtailment in China *Renew. Sustain. Energy Rev.* **105** 476–86

Reichenberg L, Hedenus F, Mattsson N and Verendel V 2022 Deep decarbonization and the supergrid—prospects for electricity transmission between Europe and China *Energy* **239** 122335

Reichenberg L, Hedenus F, Odenberger M and Johnsson F 2018 The marginal system LCOE of variable renewables—evaluating high penetration levels of wind and solar in Europe *Energy* **152** 914–24

Roques F, Hiroux C and Saguan M 2010 Optimal wind power deployment in Europe-A portfolio approach *Energy Policy* **38** 3245–56

Schill W-P, Pahle M and Gambardella C 2017 Start-up costs of thermal power plants in markets with increasing shares of variable renewable generation *Nat. Energy* **2** 1–6

Schindler D, Behr H D and Jung C 2020 On the spatiotemporal variability and potential of complementarity of wind and solar resources *Energy Convers. Manage.* **218** 113016

Schmidt O and Staffell I 2023 *Monetizing Energy Storage: A Toolkit to Assess Future Cost and Value* (Oxford University Press) (https://doi.org/10.1093/oso/9780192888174.001.0001)

Sepulveda N A, Jenkins J D, de Sisternes F J and Lester R K 2018 The role of firm low-carbon electricity resources in deep decarbonization of power generation *Joule* **2** 2403–20

Solomon A A, Child M, Caldera U and Breyer C 2020 Exploiting wind-solar resource complementarity to reduce energy storage need *AIMS Energy* **8** 749–770

Staffell I and Green R 2014 How does wind farm performance decline with age? *Renew. Energy* **66** 775–86

Staffell I and Pfenninger S 2016 Using bias-corrected reanalysis to simulate current and future wind power output *Energy* **114** 1224–39

Ueckerdt F, Hirth L, Luderer G and Edenhofer O 2013 System LCOE: what are the costs of variable renewables? *Energy* **63** 61–75

Villamor L V, Avagyan V and Chalmers H 2020 Opportunities for reducing curtailment of wind energy in the future electricity systems: insights from modelling analysis of Great Britain *Energy* **195** 116777

Way R, Ives M C, Mealy P and Farmer J D 2022 Empirically grounded technology forecasts and the energy transition *Joule* **6** 2057–82

Xia F, Lu X and Song F 2020 The role of feed-in tariff in the curtailment of wind power in China *Energy Econ.* **86** 104661

Zerrahn A and Schill W P 2017 Long-run power storage requirements for high shares of renewables: review and a new model *Renew. Sustain. Energy Rev.* **79** 1518–34

Zerrahn A, Schill W and Kemfert C 2018 On the economics of electrical storage for variable renewable energy sources *Eur. Econ. Rev.* **108** 259–79